Structural and functional remodeling of mitochondria as an adaptive response to energy deprivation

Andrey V. Kuznetsov[a,b,*], **Sabzali Javadov**[c], **Raimund Margreiter**[d], **Michael Grimm**[a], **Judith Hagenbuchner**[e], **Michael J. Ausserlechner**[b,**]

[a]Cardiac Surgery Research Laboratory, Department of Cardiac Surgery, Innsbruck Medical University, Innsbruck, Austria

[b]Department of Pediatrics I, Medical University of Innsbruck, Innsbruck, Austria

[c]Department of Physiology, School of Medicine, University of Puerto Rico, San Juan, PR, USA

[d]Department of Visceral, Transplant and Thoracic Surgery, Medical University of Innsbruck, Innsbruck, Austria

[e]Department of Pediatrics II, Medical University of Innsbruck, Innsbruck, Austria

Abstract

Cancer cells bioenergetics is more dependent on glycolysis than mitochondrial oxidative phosphorylation, a phenomenon known as the Warburg Effect. It has been proposed that inhibition of glycolysis may selectively affect cancer cells. However, the effects of glycolysis inhibition on mitochondrial function and structure in cancer cells are not completely understood. Here, we investigated the comparative effects of 2-deoxy-D-glucose (2-DG, a glucose analogue, which suppresses cellular glycolysis) on cellular bioenergetics in human colon cancer DLD-1 cells, smooth muscle cells, human umbilical vein endothelial cells and HL-1 cardiomyocytes. In all cells, 2-DG treatment resulted in significant ATP depletion, however, the cell viability remained unchanged. Also, we did not observe the synergistic effects of 2-DG with anticancer drugs doxorubicin and 5-fluorouracil. Instead, after 2-DG treatment and ATP depletion, mitochondrial respiration and membrane potential were significantly enhanced and mitochondrial morphology changed in the direction of more network organization. Analysis of protein expression demonstrated that 2-DG treatment induced an activation of AMPK (elevated pAMPK/AMPK ratio), increased mitochondrial fusion (mitofusins 1 and 2) and decreased fission (Drp1) proteins. In conclusion, this study suggests a strong link between respiratory function and structural

[*]Correspondence to: A.V. Kuznetsov, Cardiac Surgery Research Laboratory, Department of Cardiac Surgery, Innsbruck Medical University, Innsbruck, Austria. andrey.kuznetsov@tirol-kliniken.at. [**]Corresponding author. michael.j.ausserlechner@i-med.ac.at (M.J. Ausserlechner).

organization of mitochondria in the cell. We propose that the functionality of the mitochondrial network is enhanced compared to disconnected mitochondria.

Keywords

Cancer cells; Cellular ATP; 2-deoxy-D-glucose; Energy stress; Glucose metabolism; Mitochondria; Mitochondrial function; Mitochondrial dynamics/network; Mitochondrial membrane potential

1. Introduction

Adenosine triphosphate (ATP), which provides the energy for the maintenance of vital functions of the cell, is formed through the two tightly regulated processes, glycolysis and mitochondrial oxidative phosphorylation (OXPHOS). However, the crosstalk between these processes has not yet been completely understood and requires further studies. Particularly, little is known about what triggers the shift between glycolysis and OXPHOS. Mitochondrial bioenergetics is a more efficient metabolic process for ATP synthesis in comparison to glycolysis. In oxidative and high energy-consuming cells and tissues (cardiomyocytes, soleus muscles, etc.) cellular energy metabolism relies on the mitochondrial OXPHOS. In contrast, cancer cells use glycolysis as a main source of ATP (known as the Warburg effect [1,2]), especially, under hypoxic conditions, although mitochondria also were found to be involved in carcinogenesis. Hence, a potential role of mitochondria in cancer bioenergetics had received renewed interest [3–5]. OXPHOS has been shown to be upregulated in several cancer cell types, suggesting the mitochondria as a target for cancer therapy [6–10].

The key enzyme catalyzing the first step of the glycolytic pathway, hexokinase is highly expressed in malignant cells compared to normal cells [11,12] underlying the necessity of high glycolytic metabolism for the maintenance of sufficient ATP levels in cancer cells. The high dependence of cancers on glycolysis indicates a rationale for anti-tumor therapy by targeting glycolysis. Accordingly, several studies proposed that inhibition of glycolysis by various inhibitors such as 2-deoxy-D-glucose (2-DG), which inhibits the first step in the glycolysis (hexokinase), as well as jasmonates, 3-bromo-pyruvate (3-BrPA) and 6-aminonicotinamide (6-AN, an inhibitor of G-6-PD) can selectively affect cancer cells by the depletion of cellular ATP [13–16]. The possible effects of glycolysis inhibitors on mitochondrial function and structure have not yet been sufficiently investigated. On the other hand, several studies suggested that OXPHOS can also be upregulated in cancer cells (reverse Warburg effect) [6–8], and targeting mitochondria through inhibition of OXPHOS may have therapeutic potential for cancer treatment [6,9]. Therefore, understanding the crosstalk mechanisms between glycolysis and OXPHOS [17] can be helpful for the development of new anticancer agents that could target mitochondria and glycolysis with high selectivity. In addition, targeting glycolysis suggested against the chemoresistance of cancer cells to various anticancer drugs [15,16,18]. Mitochondrial dysfunction has been proposed to play a role in the development of chemoresistance in cancer [16].

This study attempts to simultaneously elucidate the structural and functional changes that occur in mitochondria of different cell types in response to 2-DG treatment that causes ATP depletion [19]. Results demonstrate that mitochondrial respiration and membrane potential

are remarkably improved by the 2-DG treatment specifically in cancer DLD-1 cells. The improved mitochondrial function was concurrent with significant changes in mitochondrial network (fusion-fission machinery), and AMPK activation.

2. Materials and methods

2.1. Cells

Human colon carcinoma DLD-1 cells, smooth muscle cells (SMC), human umbilical vein endothelial cells (HUVEC), and HL-1 cardiomyocytes were used in this study, but in respirometry and imaging studies we were more focused on cancer DLD-1 cells. DLD-1 cells were routinely cultured in RPMI-1640 growth medium supplemented with antibiotics, glutamine, and 10% FCS. SMC were grown using Medium 231 ("Sigma") + SMGs, HUVEC using EGM-2 medium ("Lonza") supplemented with 10% FCS. HL-1 cells with cardiac phenotype were grown in fibronectin–gelatine coated flasks containing Claycomb medium [20] supplemented with 10% fetal bovine serum, 100 U/ml penicillin, 100 μg/ml streptomycin, 2 mM L-glutamine and 0.1 mM norepinephrine. Cells were cultured at 37 °C and 5% CO_2. Cells were then detached with trypsin, washed, re-suspended in the growth medium ($1-2 \times 10^6$ cells/ml), and used for further analysis. In confocal imaging experiments, control cells ($20-50 \times 10^3$ cells/ml), or cells incubated with 16 mM 2-DG using LAB-TEK® chambered microscopic cover-glasses ("Nalge Nunc International", Naperville, USA). Usually, new cultures were re-established from frozen stocks every three months. Once a month routine tests were conducted to confirm that cells were free of mycoplasm (Mycoplasm Detection kit, Stratagene, Amsterdam, Netherlands). All chemical reagents were purchased from "Sigma" (Vienna, Austria).

2.2. Cell size, count and viability

Casy®−1 Cell Counter and Analyzer System model TT (Schärfe System, Reutlingen, Germany) were used to measure cell size profiles (cell count versus cell size), maximal and mean values of cell diameters and volumes, as well as cell viability. For this purpose, 100 μl of cell suspension was added to 10 ml of measuring buffer. In addition, a routine Trypan Blue (0.05%) test was used to count viable and non-viable cells. Trypan Blue exclusion of suspended control cells was >95%. After 48 h of incubation with 2-DG, the percentage of all Trypan Blue excluding cells was not decreased as compared with controls. Similarly, the percentage of unstained cells in suspension was not different from controls after 2-DG treatment.

2.3. Cellular ATP determination in various cell lines

Cellular ATP content was measured in control cells and after 2-DG treatment, using the luciferin-luciferase system (bioluminescent cell assay kit, "Sigma") and multiplate luminometer. ATP was extracted from cells after protein precipitation using 0.5 M perchloric acid and subsequent neutralization with 1 M KCO3 and 100 mM HEPES, following centrifugation at 10,000 g for 5 min to remove precipitates. The ATP calibration curve (0–1.5 μM) was used for the final analysis.

2.4. Determination of the mitochondrial respiratory function

Oxygen consumption of the cells (usually $1–3 \times 106$ cells/ml) was measured by high resolution respirometry [21] using a titration-injection respirometer (Oroboros® Oxygraph, Innsbruck, Austria) in the growth medium RPMI-1640 (for DLD-1 cells), or Claucomb (for HL-1 cells) before and after addition of the mitochondrial uncoupler FCCP (2–4 μM) at 37 °C, assuming an O_2 solubility of 10.5 μmol*L-1*kPa-1 (1.4 μmol*L-1*mmHg-1). DatLab software (Oroboros, Innsbruck, Austria) was used for data acquisition and analysis. Respiration rates were expressed in pmol of O_2 per second, per 10^6 cells. Both basal (endogenous) and uncoupled respiration rates were linearly dependent on the cell density in a range of $0.1–6.0 \times 10^6$ cells/ml. Also, mitochondria-specific inhibitors blocked respiration confirming that oxygen consumption was due to the mitochondrial respiratory chain.

2.5. Enzymatic analysis

The activity of citrate synthase, which is localized in the mitochondrial matrix, was analyzed as a marker for mitochondria in cell lysates that were frozen in liquid nitrogen and stored at −80 °C. The activity of the enzyme was determined spectrophotometrically at 30 °C by measuring coenzyme A formation at 412 nm in medium supplemented with 0.1% Triton X-100.

2.6. Flow cytometry flow analysis

Flow cytometry of control cells and after treatment with 2-DG (20 mM) was used for the analysis of the changes in Ψ_m in the cells loaded with TMRM (0.1 μM), as Ψm-sensitive fluorescent indicator (see also confocal microscopy part below), applying the Becton Dickinson Cytometry System and CellQuest software. For each analysis, 20,000–30,000 gated events were collected.

2.7. Confocal fluorescent imaging of mitochondria

Mitochondrial distribution, morphology and structural arrangement were analyzed by confocal microscopy as described previously [22–25]. Briefly, cells were plated in Lab-Tek chambered coverglass (Nalge Nunc, Rochester, NY) with chamber volumes of 0.3 ml (~50 × 10^3 cells per chamber). In order to analyze the intracellular mitochondrial arrangement and changes in mitochondrial morphology, distribution, and Ψ_m after 2-DG treatment, cells were incubated for 30 min at room temperature in serum-free culture medium containing 50–100 nM tetramethylrhodamine methyl ester (TMRM, "Sigma"). TMRM is a lipophilic, cell-permeable, cationic, nontoxic, fluorescent dye that specifically stains live mitochondria. TMRM is accumulated specifically in mitochondria depending on their Ψm. TMRM fluorescence was excited with a 543-nm helium−neon laser, at a laser output power of 1 mW. The signal was redirected to a 560-nm long-pass filter and collected in a pinhole (one Airy disk unit). In separate series of experiments, cells were loaded also with another established mitochondrial specific probe MitoTracker® Green FM (0.2 μM, 45 min, Molecular Probes). Mitochondria staining in live cells were acquired with a microlens-enhanced Nipkow disk-based confocal system UltraVIEW RS (Perkin Elmer, Wellesley MA, USA) mounted on an Olympus IX-70 inverse microscope (Olympus, Nagano, Japan) with a 40 × water immersion LUMPlanFI/IR objective (NA 0.8). Image acquisition, restoration, and analysis were done

with the UltraVIEW RS software. TMRM fluorescence was colocalized with mitochondrial flavoproteins, integral components of the mitochondrial inner membrane. Notably, both TMRM and Mitotracker Green at concentrations used in this study had no effect on cell dynamics and viability over a long time.

2.8. Western blot analysis

DLD-1 cells were homogenized on ice in NP-40 lysis buffer [50 mM Tris-HCl (pH 8.0), 150 mM NaCl, 0.02% Na-Azide, 0.1% SDS, 1.0% NP-40, 0.5% Na-deoxycholate, 10 mM Na-orthophosphate, 25 mM glycero-2-phosphate, 25 mM NaF, supplemented with 1 mM PMSF, 0.2 mM Na-orthovanadate and proteinase inhibitor cocktail (Calbiochem)]. Insoluble material was removed by centrifugation at 4 °C and protein concentration was determined in the supernatant using the BCA-Assay (Pierce) with bovine serum albumin as standard. Blotting was performed at 400 mA for 60 min at 4 °C. The membrane was blocked for 1 h in TBS supplemented with 0.05% Tween 20 (vol/vol) and 5% (wt/vol) nonfat dry milk (Company). Incubation with the primary antibody ("Abcam") against appropriate proteins, diluted in TBS supplemented with 0.05% Tween 20 (vol/vol) and 5% (wt/vol) dry milk powder was carried out either at room temperature or overnight at 4 °C. After three washes (10 min each) with TBS containing 0.05% Tween 20 (wt/vol), the blot was incubated with the anti-rabbit horseradish peroxidase-linked secondary antibody ("Abcam") diluted 1:3000 in TBS supplemented with 0.05% Tween 20 (vol/vol) and 1.6% (wt/vol) dry milk powder for 45 min at room temperature. Following three washes the bands were visualized using the enhanced chemiluminescence detection system (ECL, Amersham).

2.9. Statistical analysis

Data were analyzed using t-test. All data are presented as means $\pm$ SD. $P \quad 0.05$ was considered statistically significant.

3. Results

3.1. Cellular ATP depletion by 2-DG

The initial metabolic step in glycolysis and glycolytic cellular ATP production is the hexokinase with the transformation of glucose to glucose-6-phosphate. A non-metabolizable glucose analogue, 2-DG suppresses glycolysis, leading to the depletion of cellular ATP. In our study, incubation with 2-DG significantly reduced ATP levels in various cells.

As shown in Figs. 1, 2-DG treatment during 48 h or 72 h decreased the level of cellular ATP to 30–60% of control in all cells including human carcinoma DLD-1 cells, HL-1 cells derived from mouse atrial cardiomyocytes (HL-1 cells [20] apparently are more dependent on glycolytic energy production), human umbilical vein endothelial cells (HUVEC), and smooth muscle cells (SMC). It was found that 2-DG at a concentration of 16 mM is optimal for the maximum effect. ATP depletion was more pronounced in DLD-1 cells (to 32% of controls) as compared with HL-1 (48%), SMC (52%), and HUVEC (59%). This may reflect higher sensitivity of cancer cells to inhibition of glycolysis in comparison with non-cancer cells (due to the Warburg effect). In SMC, 72-h treatment with 2-DG resulted in equal ATP depletion as compared with 48 h. 2-DG it was even less effective in HL-1 cells. However,

72-h treatment produced a less pronounced effect compared with 48-h treatment in DLD-1 and HUVEC cells. This may be associated with high adaptive activities of mitochondria (*see* mitochondrial respiration section) and therefore, it could be more ATP generation due to OXPHOS and, as a result, higher ATP cellular levels in these cells after sustained incubation.

3.2. Cell size/viability

No changes in the DLD-1 colon carcinoma cell viability have been detected after 2-DG treatment (95–99% of control), despite glycolysis inhibition and significant ATP depletion (Fig. 1). Similarly, no changes in cell viability have been detected applying other glycolysis inhibitors (48 h incubation) such as brome-pyruvate (10–20 μM) or jasmonate (50 μM). Cell size profiles (cell count versus cell size) analyzed by the Casy® Cell Counter and Analyzer System showed no changes in cell viability and cell size distribution after 48 h incubation with 16 mM 2-DG. The cell diameter was 17.2 ± 0.9 μm and 17.1 ± 0.2 μm in control and 2-DG-treated DLD-1 cells, respectively. Similarly, no effects of 48 h of incubation with the 2-DG on cell size have been detected in HL-1 cells, HUVEC, and SMC (*data not shown*). In addition, cell damage was qualitatively estimated by a routine Trypan Blue staining test to count viable and non-viable cells (99 ± 2% of control). No changes in cell size have been observed also after incubation with other glycolysis inhibitor jasmonate. Furthermore, in DLD-1 cells, 2-DG treatment (16 mM) in combination with doxorubicin (DOX, 10 μg/ml) had no additional effects on the cell size and cell viability. Cell diameter was 17.1 ± 0.8 μm (viability 97–99%) for control, 17.5 ± 0.5 μm (viability 46 ± 4%) for DOX-treated cells, and 16.9 ± 0.5 μm (viability 48 3%) for cells treated simultaneously with DOX and 2-DG.

3.3. Cell respiration

Changes in mitochondrial function were measured in cultured cells (mostly DLD-1 cancer cells) by the high-resolution respirometer (oxygraph). The most interesting and unexpected results were obtained from the analysis of the 2-DG effects on the mitochondrial respiration; inhibition of glycolysis and ATP depletion (energy stress) were accompanied by a significant (~2 fold) increase in the mitochondrial respiratory activity. Stimulation of the mitochondrial respiration by 2-DG was concentration-dependent.

Fig. 2 shows representative experiments, demonstrating also significantly higher endogenous and uncoupled (FCCP-stimulated) mitochondrial respiration in DLD-1 cells after incubation of DLD-1 cells with 2-DG (48 h, 16 mM).

Fig. 3 demonstrates the concentration dependence of the 2-DG effect (48 h incubation) on the mitochondrial endogenous and uncoupled (FCCP) respiration. The uncoupling control ratio (UCR) was ~4.3–4.5. In each separated experiment, a specific FCCP titration protocol was applied for the assessment of the optimal FCCP concentration. Importantly, endogenous and uncoupled respirations were linearly dependent on the cell density in a range of $0.2–6.0 \times 10^6$ cells/ml.

3.4. Changes in mitochondrial membrane potential

Fluorescence flow cytometry analysis was applied to the estimation of changes in Ψ_m, using Ψ_m-sensitive fluorescent probe TMRM (50 nM). As a negative control, in each measurement, we used uncoupling of mitochondria by 4 μM FCCP and 10 μM antimycin A that led to the complete collapse of Ψ_m.

We found a significant increase in averaged TMRM fluorescence signal in DLD-1, SMC, and HL-1 cells after incubation with 16 mM 2-DG for 48 h (Fig. 4). Interestingly, among all cells used in the study, no effect of 2-DG on the Ψ_m has been observed only in HUVEC. Results showed that 2-DG treatment resulted in a significant shift of the fluorescence intensity distribution peak, pointing to the increase in the Ψ_m (Fig. 4). Notably, selective cellular (not mitochondrial [26]) membrane permeabilization by digitonin (50 μg/ml) had no effect on the measured TMRM fluorescence signal. In some cases, two cell subpopulations with normal and elevated TMRM fluorescence cell count/distribution could be seen after 2-DG treatment. The significant increase of fluorescence signals after 2-DG treatment as an indicator of elevated Ψ_m can be interconnected with activated mitochondrial respiratory function. In addition, we observed no effects of the AMPK activator, AICAR (1 mM) on the Ψ_m.

3.5. Citrate synthase activity

Assessment of the activity of the mitochondrial matrix enzyme citrate synthase is frequently used as a mitochondrial marker and an indicator of mitochondrial mass/amount, due to its rather stable activity. In all cell lines, no effect of 2-DG treatment (16 mM, 48 h of incubation) on citrate synthase activity has been found, indicating no changes in mitochondrial mass/quantity (Table 1).

3.6. Mitochondrial morphology/organization

To analyze intracellular mitochondrial morphology/arrangement and their changes in energy stress and ATP depletion after 2-DG treatment, fluorescent confocal imaging of mitochondria has been used. Cell and mitochondria were preloaded with specific fluorescent mitochondrial probes, TMRM (red, 0.1 μM, 30 min) and MitoTracker Green (green, 0.2 μM, 45 min). Mitochondria in merge images (TMRM/Mito-Tracker) can be seen in yellow color (Fig. 5).

The Fig. 5A shows the remarkable differences in mitochondrial structure and organization in DLD-1 cells that result from incubation with 2-DG (48 h, 16 mM). It can be clearly seen the appearance of the more mitochondrial network, as compared with more separated mitochondria in the control cells. In contrast, no effects of 2-DG on mitochondrial structure were found in HL-1, HUVEC, and SMC cells (Fig. 5B–D). (These cells had mitochondrial networks already in the controls).

3.7. Mitochondrial fusion-fission proteins and AMPK

For elucidation of the potential role of mitochondrial fusion-fission proteins, and AMPK in respiration and structural organization of mitochondria in response to 2-DG treatment, we determined the expression of these proteins. As shown in Fig. 6, 2-DG treatment increased

protein levels of the fusion proteins, mitofusin 1 (Mfn1) and 2 (Mfn2) but decreased the fission protein, Drp1 in DLD-1 cells. However, these effects were not observed in HUVEC and SMC, thus, demonstrating a difference (different response to 2-DG) between normal and cancer cells (*data not shown*). Analysis of AMPK, which is tightly involved in cellular bioenergetics as a cellular energy sensor, demonstrated negligible changes (statistically no significant) in the p-AMPK to total AMPK ratio after 48 h of incubation with 16 mM 2-DG.

However, a remarkable activation of AMPK has been seen after 72 h as evidenced by increased p-AMPK levels (Fig. 7). Interestingly, we observed no effects of the AMPK activator AICAR at 1 mM after incubation for 60 min (suppl. Fig. 1). Also, we were not able to observe any noticeable effects of AICAR on the endogenous, FCCP and 2-DG-stimulated mitochondrial respiration as well as the mitochondrial structure/organization (*data not shown*).

4. Discussion

The balance between glycolysis and mitochondrial OXPHOS in cells depends on the conditions (stimuli) [17] and can be strongly variable depending on the tissue/cell type. For example, inhibition of OXPHOS during hypoxia or ischemia leads to the remarkable activation of glycolysis [27,28]. Similarly, it has been suggested that inhibition of glycolysis activates mitochondrial function [29,30]. Cancer cells are mostly glycolytic with less participation of OXPHOS in energy metabolism, however, many studies revealed that mitochondria also participate in ATP supply during tumorigenesis [29,30]. Comparative analysis in tumor and normal cells generally demonstrates a decrease in mitochondrial OXPHOS capacity. However, the mechanism of crosstalk between glycolysis and OXPHOS in cancer cells remain unclear. Recent studies suggested that inhibition of glycolysis can specifically abolish cancer cells, and that the different responses of cancer cells and normal cells to ATP deprivation and energy stress may be useful for the development of new cancer therapy strategies [15,16]. Moreover, it has been proposed that this approach may help to overcome the phenomenon of chemoresistance and may, therefore, provide a promising biochemical basis for better therapy [6,16,31,32]. So, in order to test these hypotheses, we used 2-DG treatment and consequent ATP depletion in different cancer and normal cell lines. Despite significant ATP depletion, we observed no effect of 2-DG on the cell viability and size in all cells involved in our study. Likewise, inhibition of glycolysis by 2-DG, in combination with the anticancer drugs doxorubicin or 5-fluorouracil had no additional effects on the cell viability ("Results"). These observations are not consistent with the suggestions that inhibition glycolysis is useful for overcoming the chemoresistance.

We sought to elucidate the ability of glycolysis inhibition to increase OXPHOS via adaptation and remodeling of mitochondria. We found a significant elevation of mitochondrial respiratory function in DLD-1 cancer cells (Figs. 2, 3) at rather constant mitochondrial mass/amount as evidenced by the activity of citrate synthase (Table 1). This effect could be explained, at least in part, by activation of mitochondrial respiratory chain complexes. In addition, elevated respiratory capacity was accompanied by the increase in Ψ_m assessed by the flow cytometry technique. These data suggest that in response to cellular energy requirements, the activation of mitochondrial bioenergetics may compensate

ATP depletion induced by suppression of glycolysis [29]. Moreover, glucose deprivation in cancer cells, as well as hypoxia and 2-DG-induced stress and cytotoxicity may change cellular metabolism [16]. It has been shown that 2-DG may change the effector functions of various cells (e.g. human T cells [33]).

It has been shown that a reduction in the lactate dehydrogenase A (LDH-A) activity may also result in stimulation of mitochondrial respiratory function with a simultaneous decrease of mitochondrial Ψ_m (Valeria R. Fantin, 2006 [34]). Although glycolysis inhibition by 2-DG (ATP depletion, Fig. 1) and elevated respiration at reduced LDH-A activity might have different mechanisms/effects on mitochondrial bioenergetics and function. However, in contrast, we observed increased Ψ_m (*see* Results).

Through fission and fusion, mitochondrial morphology can change from small spheres or short rods to long tubules forming large network-like structures within the same cell. It is now generally accepted that high mitochondrial function can be achieved through the balance between processes of fusion and fission of these organelles. Moreover, mitochondrial quality control in the cell is realized by selective elimination of damaged or defective mitochondria through autophagy (mitophagy) (*reviewed in* O. Shirihai, 2013 [35–38] and B. Westermann 2012 [39,40]). The mitochondrial quality control is achieved by the dynamic interplay between fission-fusion, selective mitophagy and mitochondrial biogenesis which might be controlled by Ψ_m. It has been suggested that the changes in mitochondrial structure/organization (remodeling) are involved in the mechanism of their adaptation to metabolic demands. This provides a link between mitochondrial dynamics and the balance of energy demand/supply, thus, regulating bioenergetic efficiency and mitochondrial OXPHOS capacity (Shirihai, 2008, 2013 [35–37]). Therefore, numerous studies suggest the existence of a relationship between mitochondrial biogenesis, function and structure/morphology, and cellular arrangement in various cells (muscles, beta cells, human fibroblasts, COS-7, etc.) (*reviewed in* M. Liesa, O. Shirihai; M. Picard, O. Shirihai [35,36], and G. Benard 2007, 2008 [41,42]). In response to cellular and environmental stresses, mitochondria undergo morphology transitions regulated by fusion and fission. These events of mitochondrial dynamics are central regulators of cellular activity, but the mechanisms linking mitochondrial shape to cell function remain unclear. Mitochondrial dynamics precisely adjust the main functions of mitochondria, including signaling under conditions of metabolic changes [35,36].

Analysis of the effects of energy substrates on mitochondrial function, morphology and structure, and their ability to regulate the balance of the glycolysis and OXPHOS was assessed in human cancer cell line (HeLa) to clarify whether all these changes can be reversible (Rossignol R. 2004 [43]). These studies demonstrated a complex and joint response of mitochondria to substrates availability. Likewise, the activation of mitochondrial respiration due to a change in the glycolytic ATP availability shown in our study was concomitant with structural alterations in the direction of the more mitochondrial network in DLD-1 cells (Fig. 5). These observations indicate that there is a strong link between the mitochondrial organization and mitochondrial respiratory activity, suggesting a shift in the balance between fusion and fission toward enhanced mitochondrial fusion (Fig. 5A). It is well known that the two Fzo homologs proteins, Mfn1 and Mfn2 participate

in the mitochondrial fusion machinery [44–48]. To further investigate the effects of structural mitochondrial changes under energy stress and ATP depletion, we analyzed the expression of Mfn1 and Mfn2, together with the analysis of Drp1, a fission protein [49,50]. We found that 2-DG treatment induced a significant upregulation of Mfn1 and Mfn2, concomitant with down-regulation of Drp1 (Fig. 6A, B). These results are in full accordance with previous oxygen-glucose deprivation experiments [28], with findings from survivin-overexpressing cells [51], as well as with our imaging results (Fig. 5). Moreover, previous studies showed that Drp1 knockout in pancreatic cancer cells diminishes energy status and mitochondrial activity [50]. Interestingly, no effects (or slightly opposite effects) of 2-DG treatment on the expression of fusion-fission proteins (Mfn1, Mfn2, and Drp1) or activation of AMPK were found in the non-cancer cell lines, HUVEC, and SMS. These data indicate significant differences between cancer and normal cells. Based on these findings, we can suggest that the mitochondrial network in cancer cells can functionally be more active than that in separated mitochondria. These observations could be in line with the suggestion that mitochondrial fusion is predominantly essential in cells of high respiratory activities [39]. This permits the distribution of several metabolic and mitochondrial components in the mitochondrial networks for the optimization of their tasks, working also against accumulation of mutations [39,40]. Moreover, mitochondrial fragmentation (fission) has been shown to be an early sign of apoptosis [35,52,53], with possible decline also in the functional activity of mitochondria. Although this point was not sufficiently studied, cytochrome *c* depleted mitochondria would be certainly less active [21] and, on the other hand, cytochrome *c* release is well known as an important factor in the apoptosis activation and can be elevated during fission. Mitochondria in Mfn1-deficient cells have been shown to lose their Ψ_m, while the fusion of mitochondria appears to permit cooperation between separated mitochondria and, in that way, defend the organelles from their dysfunction [44]. Correspondingly, several Mfn2 ablation experiments have demonstrated a mitochondrial dysfunction, oxidative stress, as well as repression of nuclear-encoded subunits of respiratory chain complexes [54–56]. Our study is the first analysis of the changes that occur in the structure/organization and the main functional properties of mitochondria during 2-DG treatment, causing energy stress and glycolytic ATP depletion.

In addition, our results show that AMPK (a critically important cellular energy sensor [57–59]), has been activated after 72 h of 2-DG treatment (Fig. 7) with the appearance of increased p-AMPK/AMPK ratio associated with increased levels of p-AMPK. However, AICAR, AMPK activator, which is converted into 5-Aminoimidazole-4-carboxamide-1-b-D-Ribofuranosyl-monophosphate (ZMP), the direct allosteric activator of phospho-transferase activity [60] had no effects neither on respiration nor structure of mitochondria. Notably, the effects of AICAR have been suggested to be more apparent in primary cells than in rapidly proliferating cells, including cancer cells [61]. Therefore, the effects of direct AMPK activators such as A-769662, which, unlike AICAR, possess high specificity toward AMPK and allosterically activates it without phosphorylation of Thr172 [62,63] might be interesting to evaluate. The activation of AMPK after 2-DG treatment is in line with 2-DG-provoked ROS production and AMPK activation induced by the 2-DG treatment of bovine aortic endothelial cells, which can be blocked by siRNA-mediated knockdown of AMPK, with a general conclusion that AMPK can be needed for the ROS-activated

autophagy in energy depletion and cell stress experiments [64]. The molecular basis of all these phenomena is not clearly understood. However several suggestions can be proposed, including the certain participation of mitochondrial fusion-fission proteins and cellular AMPK activation. Finally, respirometry, together with confocal fluorescent imaging analysis of mitochondrial morphology/organization (networks) and analysis of fusion-fission protein expression, provides the evidence of close-fitting connections between the mitochondrial organization and their respiratory capacity.

5. Conclusions

Our studies show that when glycolysis is inhibited by 2-DG treatment with further ATP deprivation and energy stress, the proper viability of cancer and other cells remains intact, but functional (OXPHOS) and structural (morphology/organization) properties of mitochondria substantially changed with a shift to the higher respiration capacities and more mitochondrial network organization. This study demonstrates that crosstalk exists between structural reorganization and functional remodeling of mitochondria in response to 2-DG treatment as a result of adaptation of cancer cells to the energy depletion. Although the precise molecular mechanisms of these interconnections are still not clear and require further investigation, mitochondrial dynamics proteins and AMPK are apparently involved in these mechanisms. The main question on whether the dynamic structure of the mitochondria is remodeled due to a higher OXPHOS activity, or rather a specific mitochondrial structure (networks) possesses a higher mitochondrial respiratory capacity remains unanswered. Based on our findings presented in this study, we can suggest that the specific changes structure can lead to the functional activation. Future studies are needed to establish a cause-and-effect relationship between structural and functional remodeling of mitochondria in response to energy deprivation in cancer cells.

Supplementary Material

Refer to Web version on PubMed Central for supplementary material.

Acknowledgments

Abbreviations:

AMPK	AMP-activated protein kinase
AICAR	5-aminoimidazole-4-carboxamide-1-b-D-ribofuranosyl
2-DG	2-deoxy-D-glucose
Drp1	dynamin-related protein 1

HUVEC	human umbilical vein endothelial cells
FCCP	*p*-trifluoromethoxyphenylhydrazone
Mfn1	mitofisin 1
Mfn2	mitofisin 2
SMC	smooth muscle cells
TMRM	tetramethylrhodamine methyl ester

References

[1]. Warburg O, On respiratory impairment in cancer cells, Science 124 (1956) 269–270. [PubMed: 13351639]

[2]. Zheng J1, Energy metabolism of cancer: glycolysis versus oxidative phosphorylation, Oncol Lett 4 (6) (2012) 1151–1157. [PubMed: 23226794]

[3]. Gogvadze V, Zhivotovsky B, Orrenius S, The Warburg effect and mitochondrial stability in cancer cells, Mol. Asp. Med 31 (2010) 60–74.

[4]. Hsu PP, Sabatini DM, Cancer cell metabolism: Warburg and beyond, Cell 134 (2008) 703–707. [PubMed: 18775299]

[5]. Vander Heiden MG, Cantley LC, Thompson CB, Understanding the Warburg effect: the metabolic requirements of cell proliferation, Science 324 (2009) 1029–1033. [PubMed: 19460998]

[6]. Ghosh P, Vidal C, Dey S, Zhang L, Mitochondria targeting as an effective strategy for cancer therapy, Int. J. Mol. Sci 21 (9) (2020) 3363.

[7]. Whitaker-Menezes D, Martinez-Outschoorn UE, Flomenberg Birbe NRC, Witkiewicz AK, Howell A, Pavlides S, Tsirigos A, Ertel A, Pestell RG, Broda P, Minetti C, Lisanti MP, Sotgia F, Hyperactivation of oxidative mitochondrial metabolism in epithelial cancer cells in situ: visualizing the therapeutic effects of metformin in tumor tissue, Cell Cycle 10 (23) (2011) 4047–4064. [PubMed: 22134189]

[8]. Ertel A, Tsirigos A, Whitaker-Menezes D, Birbe RC, Pavlides S, Martinez-Outschoorn UE, Pestell Howell A, Sotgia F, Lisanti MP, Is cancer a metabolic rebellion against host aging? In the quest for immortality, tumor cells try to save themselves by boosting mitochondrial metabolism, Cell Cycle 11 (2) (2012) 253–263. [PubMed: 22234241]

[9]. Ashton TM, McKenna WG, Kunz-Schughart LA, Higgins GS, Oxidative phosphorylation as an emerging target in cancer therapy, Clin. Cancer Res 24 (11) (2018) 2482–2490. [PubMed: 29420223]

[10]. Cheng G, J., Dranka Zielonka BP, Donna McAllister D, Craig Mackinnon AG, Joseph B, Kalyanaraman J, Mitochondria-targeted drugs synergize with 2-deoxyglucose to trigger breast cancer cell death, Cancer Res 72 (10) (2012) 2634–2644. [PubMed: 22431711]

[11]. Patra KC, Wang Q, Bhaskar PT, Miller L, Wang Z, Wheaton W, Chandel N, Laakso M, Muller WJ, Allen EL, Jha AK, Smolen GA, Clasquin MF, Robey B, Hay N, Hexokinase 2 is required for tumor initiation and maintenance and its systemic deletion is therapeutic in mouse models of cancer, Cancer Cell 24 (2) (2013) 213–228. [PubMed: 23911236]

[12]. Sheng H, Tang W, Glycolysis inhibitors for anticancer therapy: a review of recent patents, Recent Pat Anticancer Drug Discov 11 (3) (2016) 297–308. [PubMed: 27087655]

[13]. Kang HT, Hwang ES, 2-Deoxyglucose: an anticancer and antiviral therapeutic, but not anymore a low glucose mimetic, Life Sci 78 (12) (2006) 1392–1399. [PubMed: 16111712]

[14]. Alves AP, Mamede AC, Alves MG, Oliveira PF, Rocha SM, Botelho MF, Maia CJ, Glycolysis inhibition as a strategy for hepatocellular carcinoma treatment? Curr. Cancer Drug Targets 19 (1) (2019) 26–40. [PubMed: 29749314]

[15]. Simons AL, Mattson DM, Dornfeld K, Spitz DR, Glucose deprivation-induced metabolic oxidative stress and cancer therapy, J. Cancer Res. Ther 5 (Suppl. 1) (2009) S2–S6. [PubMed: 20009288]

[16]. Ganapathy-Kanniappan S, Geschwind JF, Tumor glycolysis as a target for cancer therapy: progress and prospects, Mol. Cancer 12 (2013) 152, 10.1186/1476-4598-12-152. [PubMed: 24298908]

[17]. Li T, Han J, Jia L, Hu X, Chen L, Wang Y, PKM2 coordinates glycolysis with mitochondrial fusion and oxidative phosphorylation, Protein Cell 10 (8) (2019) 583–594. [PubMed: 30887444]

[18]. Guaragnella N, Giannattasio S, Moro L, Mitochondrial dysfunction in cancer chemoresistance, Biochem. Pharmacol 92 (1) (2014) 62–72. [PubMed: 25107705]

[19]. Kosic M, Arsikin-Csordas K, Paunovic V, Firestone RA, Ristic B, Mircic Petricevic AS, Bosnjak M, Zogovic N, Mandic M, Bumbasirevic V, Trajkovic Harhaji-Trajkovic L, Synergistic anticancer action of lysosomal membrane permeabilization and glycolysis inhibition, J Biol Chem 29 (44) (2016) 22936–22948, 1.

[20]. Claycomb WC, Lanson NA Jr., Stallworth BS, Egeland DB, Delcarpio JB, Bahinski A, Izzo NJ Jr., HL-1 cells: a cardiac muscle cell line that contracts and retains phenotypic characteristics of the adult cardiomyocyte, Proc. Natl. Acad. Sci. U. S. A 95 (1998) 2979–2984. [PubMed: 9501201]

[21]. Kuznetsov AV, Schneeberger S, Seiler R, Brandacher G, Mark W, Steurer W, Saks V, Usson Y, Margreiter R, Gnaiger E, Mitochondrial defects and heterogeneous cytochrome c release after cardiac cold ischemia and reperfusion, Am. J. Physiol. Heart Circ. Physiol 286 (2004) H1633–H1641. [PubMed: 14693685]

[22]. Kuznetsov AV, Hermann M, Troppmair J, Margreiter R, Hengster P, Complex patterns of mitochondrial dynamics in human pancreatic cells revealed by fluorescent confocal imaging, J. Cell. Mol. Med 14 (1–2) (2010) 417–425. [PubMed: 19382913]

[23]. Appaix F, Kuznetsov AV, Usson Y, Kay L, Andrienko T, Olivares J, Kaambre T, Sikk P, Margreiter R, Saks VA, Possible role of cytoskeleton in intracellular arrangement and regulation of mitochondria, Exp. Physiol 88 (2003) 175–190. [PubMed: 12525866]

[24]. Kuznetsov AV, Troppmair J, Sucher R, Hermann M, Saks V, Margreiter R, Mitochondrial subpopulations and heterogeneity revealed by confocal imaging: possible physiological role? Biochim. Biophys. Acta Bioenerg 1757 (2006) 686–691.

[25]. Guzun R, Gonzalez-Granillo M, Karu-Varikmaa M, Grichine A, Usson Y, Kaambre T, Guerrero-Roesch K, Kuznetsov A, Schlattner U, Saks V, Regulation of respiration in muscle cells in vivo by VDAC through interaction with the cytoskeleton and MtCK within mitochondrial Interactosome, Biochim. Biophys. Acta 1818 (6) (2012) 1545–1554. [PubMed: 22244843]

[26]. Kuznetsov AV, Veksler V, Gellerich FN, Saks V, Margreiter R, Kunz WS, Analysis of mitochondrial function in situ, in permeabilized muscle fibers, tissues and cells, Nature Prot 3 (2008) 965–976.

[27]. Opie LH, Myocardial metabolism and heart disease, Jpn. Circ. J 42 (11) (1978) 1223–1247, 10.1253/jcj.42.1223. [PubMed: 34741]

[28]. Loor G, Schumacker PT, Role of hypoxia-inducible factor in cell survival during myocardial ischemia-reperfusion, Cell Death Differ (2008) 686–690, doi: 10.1038. [PubMed: 18259200]

[29]. Maximchik P, Abdrakhmanov A, Inozemtseva E, Tyurin-Kuzmin PA, Zhivotovsky B, Gogvadze V, 2-deoxy-D-glucose has distinct and cell line-specific effects on the survival of different cancer cells upon antitumor drug treatment, FEBS J 285 (24) (2018) 4590–4601. [PubMed: 30375744]

[30]. Weber K, Ridderskamp D, Alfert M, Hoyer S, Wiesner RJ, Cultivation in glucose-deprived medium stimulates mitochondrial biogenesis and oxidative metabolism in HepG2 hepatoma cells, Biol. Chem 383 (2) (2002) 283–290. [PubMed: 11934266]

[31]. Hagenbuchner J, Oberacher H, Arnhard K, Kiechl-Kohlendorfer U, Ausserlechner MJ, Modulation of respiration and mitochondrial dynamics by SMAC-mimetics for combination therapy in chemoresistant cancer, Theranostics 9 (17) (2019) 4909–4922, 10.7150/thno.33758. [PubMed: 31410190]

[32]. Zhang L, Yang H, Zhang W, Liang Z, Huang Q, Xu G, Zhen X, Zheng LT, Clk1-regulated aerobic glycolysis is involved in glioma chemoresistance, J Neurochem 142 (4) (2017) 574–588. [PubMed: 28581641]

[33]. Renner K, et al. , Metabolic plasticity of human T cells: preserved cytokine production under glucose deprivation or mitochondrial restriction, but 2-deoxyglucose affects effector functions, Eur. J. Immunol 45 (9) (2015) 2504–2516. [PubMed: 26114249]

[34]. Fantin VR, St-Pierre J, Leder P, Attenuation of LDH-A expression uncovers a link between glycolysis, mitochondrial physiology, and tumor maintenance, Cancer Cell 9 (6) (2006) 425–434. [PubMed: 16766262]

[35]. Liesa M, Shirihai OS, Mitochondrial dynamics in the regulation of nutrient utilization and energy expenditure, Cell Metab 17 (4) (2013) 491–506, 10.1016/j.cmet.2013.03.002. [PubMed: 23562075]

[36]. Picard M, Shirihai OS, Gentil BJ, Burelle Y, Mitochondrial morphology transitions and functions: implications for retrograde signaling? Am J Physiol Regul Integr Comp Physiol 304 (6) (2013) R393–R406. [PubMed: 23364527]

[37]. Twig G, Hyde B, Shirihai OS, Mitochondrial fusion, fission and autophagy as a quality control axis: the bioenergetic view, Biochim. Biophys. Acta 1777 (2008) 1092–1097. [PubMed: 18519024]

[38]. Twig G, Elorza A, Molina AJ, Mohamed H, Wikstrom JD, Walzer G, Stiles L, Haigh SE, Katz S, Las G, Alroy J, Wu M, Py BF, Yuan J, Deeney JT, Corkey BE, Shirihai OS, Fission and selective fusion govern mitochondrial segregation and elimination by autophagy, EMBO J 27 (2008) 433–446. [PubMed: 18200046]

[39]. Westermann B, Bioenergetic role of mitochondrial fusion and fission, Biochim. Biophys. Acta 1817 (2012) 1833–1838, 10.1016/j.bbabio.2012.02.033. [PubMed: 22409868]

[40]. Westermann B, Mitochondrial fusion and fission in cell life and death, Nat. Rev. Mol. Cell Biol 11 (2010) 872–884. [PubMed: 21102612]

[41]. Benard G, Rossignol R, Ultrastructure of the mitochondrion and its bearing on function and bioenergetics, Antioxid. Redox Signal 10 (2008) 1313–1342. [PubMed: 18435594]

[42]. Benard G, Bellance N, James D, Parrone P, Fernandez H, Letellier T, Rossignol R, Mitochondrial bioenergetics and structural network organization, J. Cell Sci 120 (2007) 838–848. [PubMed: 17298981]

[43]. Rossignol R, Gilkerson R, Aggeler R, Yamagata K, Remington SJ, Capaldi RA, Energy substrate modulates mitochondrial structure and oxidative capacity in cancer cells, Cancer Res 64 (3) (2004) 985–993. [PubMed: 14871829]

[44]. Chen H, Detmer SA, Ewald AJ, Griffin EE, Fraser SE, Chan DC, Mitofusins Mfn1 and Mfn2 coordinately regulate mitochondrial fusion and are essential for embryonic development, J. Cell Biol 160 (2) (2003) 189–200. [PubMed: 12527753]

[45]. Koshiba T, Detmer SA, Kaiser JT, Chen JM, Chan DC, Structural basis of mitochondrial tethering by mitofusin complexes, Science 305 (5685) (2004) 858–862. [PubMed: 15297672]

[46]. Xie LL, Shi F, Tan Z, Li Y, Ann AM, Bode M, Cao Y, Mitochondrial network structure homeostasis and cell death, Cancer Sci 109 (12) (2018) 686–3694.

[47]. Gao S, Hu J, Mitochondrial Fusion: The Machineries In and Out. Trends Cell Biol 31 (1) (2021) 62–74, 10.1016/j.tcb.2020.09.008. [PubMed: 33092941]

[48]. Wappler Institoris EA, Dutta S, Katakam PVG, Busija DW, Mitochondrial dynamics associated with oxygen-glucose deprivation in rat primary neuronal cultures, PLoS One 8 (5) (2013), e63206, 10.1371/journal.pone.0063. [PubMed: 23658809]

[49]. Wan YY, Zhang JF, Yang ZJ, Jiang LP, Wei YF, Lai QN, Wang JB, Xin HB, Han XJ, Involvement of Drp1 in hypoxia-induced migration of human glioblastoma U251 cells, Oncol. Rep 32 (2) (2014) 619–626. [PubMed: 24899388]

[50]. Yu Meifang, et al. , Mitochondrial fusion exploits a therapeutic vulnerability of pancreatic cancer, JCI Insight 5 (16) (2019), e126915, 10.1172/jci.insight.126915.

[51]. Hagenbuchner J, Kiechl-Kohlendorfer U, Obexer P, Ausserlechner MJ, BIRC5/Survivin as a target for glycolysis inhibition in high-stage neuroblastoma, Oncogene 35 (16) (2016) 2052–2061, 10.1038/onc.2015.264. [PubMed: 26148234]

[52]. Anderson GR, Wardell SE, Cakir M, Yip C, Ahn Y-R, Ali M, Yllanes AP, Chao CA, McDonnell DP, Wood KC, Dysregulation of mitochondrial dynamics proteins are a targetable feature of human tumors, Nat. Commun 9 (1) (2018) 1677. [PubMed: 29700304]

[53]. Arismendi-Morillo G, Electron microscopy morphology of the mitochondrial network in human cancer, Int. J. Biochem. Cell Biol 41 (10) (2009) 2062–2068. [PubMed: 19703662]

[54]. Javadov S, Rajapurohitam V, Kili A, Hunter JC, Zeidan A, Faruq SN, Escobales N, Karmazyn M, Expression of mitochondrial fusion-fission proteins during post-infarction remodeling: the effect of NHE-1 inhibition, Basic Res. Cardiol 106 (2011) 99–109. . [PubMed: 20886221]

[55]. Son MJ, Kwon Y, Son M-Y, Seol B, Choi H-S, Ryu S-W, Choi C, Cho YS, Mitofusins deficiency elicits mitochondrial metabolic reprogramming to pluripotency, Cell Death Differ 22 (12) (2015) 1957–1969. [PubMed: 25882047]

[56]. Jiang S, Nandy P, Wang W, Ma X, Hsia J, Wang C, Wang Z, Niu M, Siedlak SL, Torres S, et al. , Mfn2 ablation causes an oxidative stress response and eventual neuronal death in the hippocampus and cortex, Mol. Neurodegener 13 (2018) 5, 10.1186/s13024-018-0238-8. [PubMed: 29391029]

[57]. Hardie DG, Ross FA, Hawley SA, AMPK: a nutrient and energy sensor that maintains energy homeostasis, Nat Rev Mol Cell Biol 13 (4) (2012) 251–262. [PubMed: 22436748]

[58]. Hardie DG, Hawley SA, Scott JW, AMP-activated protein kinase–development of the energy sensor concept, J. Physiol 574 (2006) 7–15. [PubMed: 16644800]

[59]. Hermann M, Kuznetsov AV, Maglione M, Margreiter R, Troppmair J, Pre-emptive strike: cytoplasmic signaling in the control of mitochondrial uproar? Cell Communication and Signaling 6 (4) (2008) 1–8. [PubMed: 18680612]

[60]. Madhavi YV, Gaikwad N, Yerra VG, Kalvala AK, Nanduri S, Kumar A, Targeting AMPK in diabetes and diabetic complications: energy homeostasis, Autophagy and Mitochondrial Health. Curr Med Chem 26 (27) (2019) 5207–5229. [PubMed: 29623826]

[61]. Kim J, Yang G, Kim Y, et al. , AMPK activators: mechanisms of action and physiological activities. Exp Mol Med 48 (2016), e224. [PubMed: 27034026]

[62]. Sanders MJ, Bronwyn AD, Heath Snowden HRMA, Carling D, Defining the mechanism of activation of AMP-activated protein kinase by the small molecule A-769662, a member of the thienopyridone family, J. Biol. Chem 282 (2007) 32539–32548. [PubMed: 17728241]

[63]. Barreto-Torres G, Hernandez JS, Jang S, Rodríguez-Muñoz AR, Torres-Ramos CA, Basnakian AG, Javadov S, The beneficial effects of AMP kinase activation against oxidative stress are associated with prevention of PPARα-cyclophilin D interaction in cardiomyocytes, Am J Physiol Heart Circ Physiol 308 (7) (2015) H749–H758. [PubMed: 25617357]

[64]. Wang Q, Liang B, Najeeb B, Shirwany A, Zou M-H, 2-deoxy-D-glucose treatment of endothelial cells induces autophagy by reactive oxygen species-mediated activation of the AMP-activated protein kinase, PLoS One 6 (2) (2011), e17234. [PubMed: 21386904]
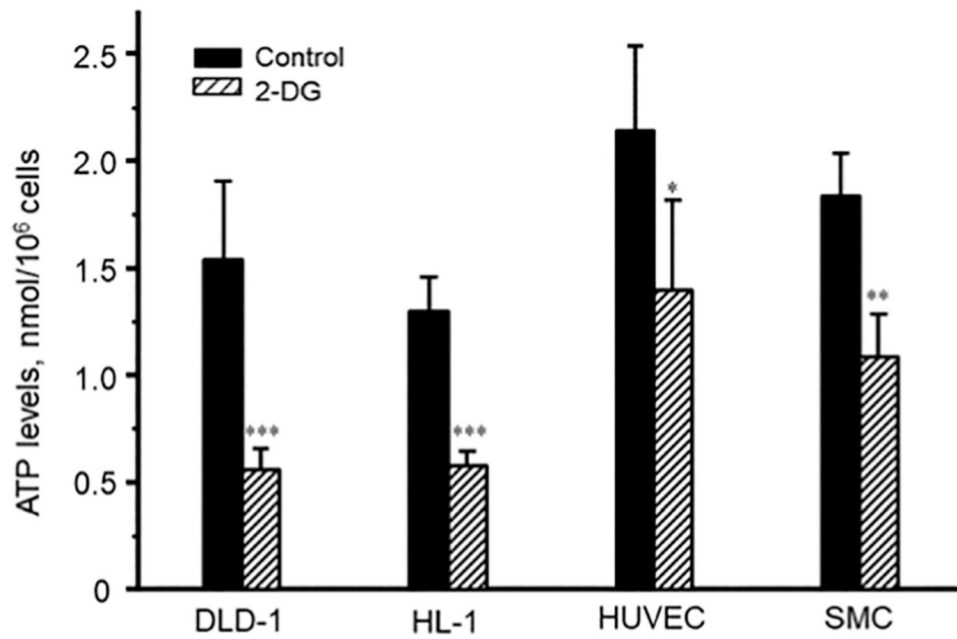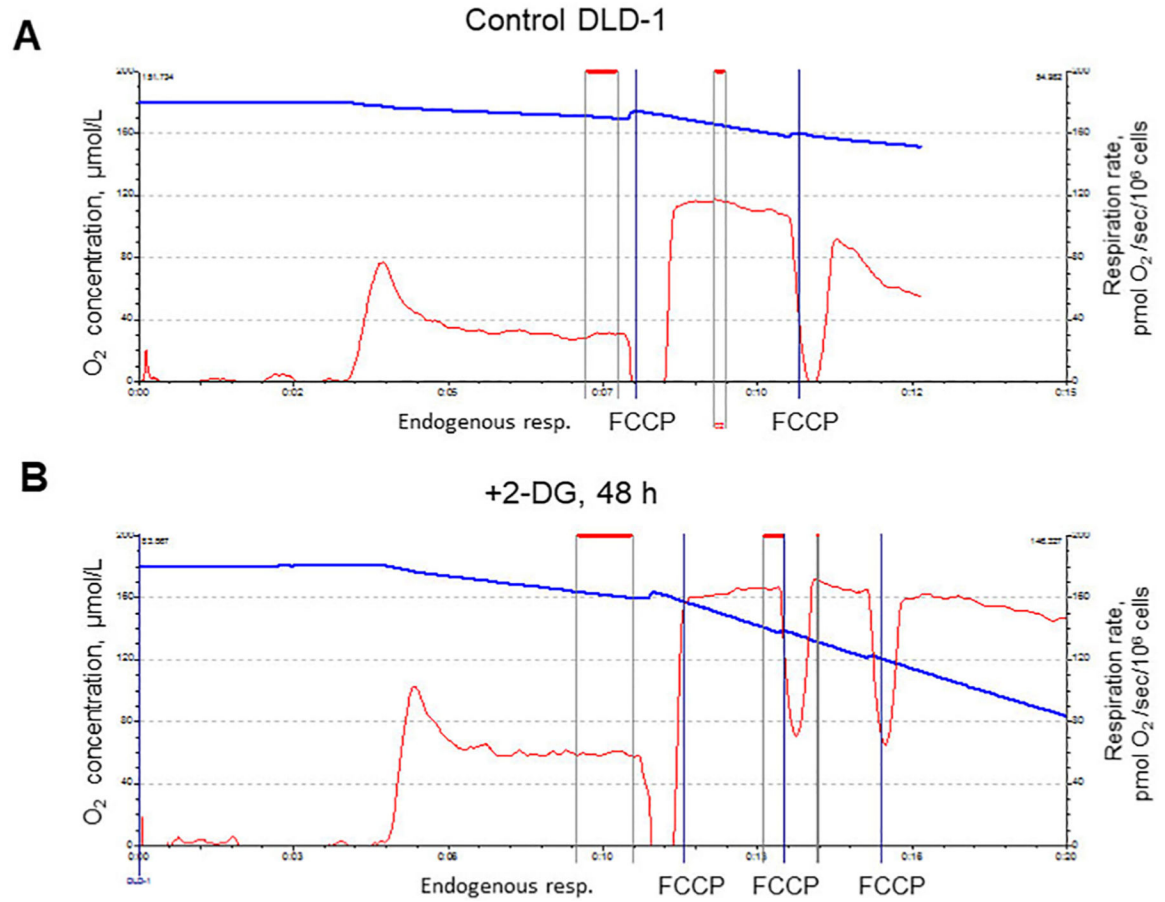
Fig. 1.
The effects of 2-DG (16 mM, 48 h) on the cellular ATP content in DLD-1, HL-1, SMC, and HUVEC cells. * $P < 0.05$; ** $P < 0.01$; *** $P < 0.001$ vs. control. $N = 3$ per group.

Fig. 2.
Respiratory activities (oxygen consumption rates) in DLD-1 cells (endogenous and uncoupled by FCCP).
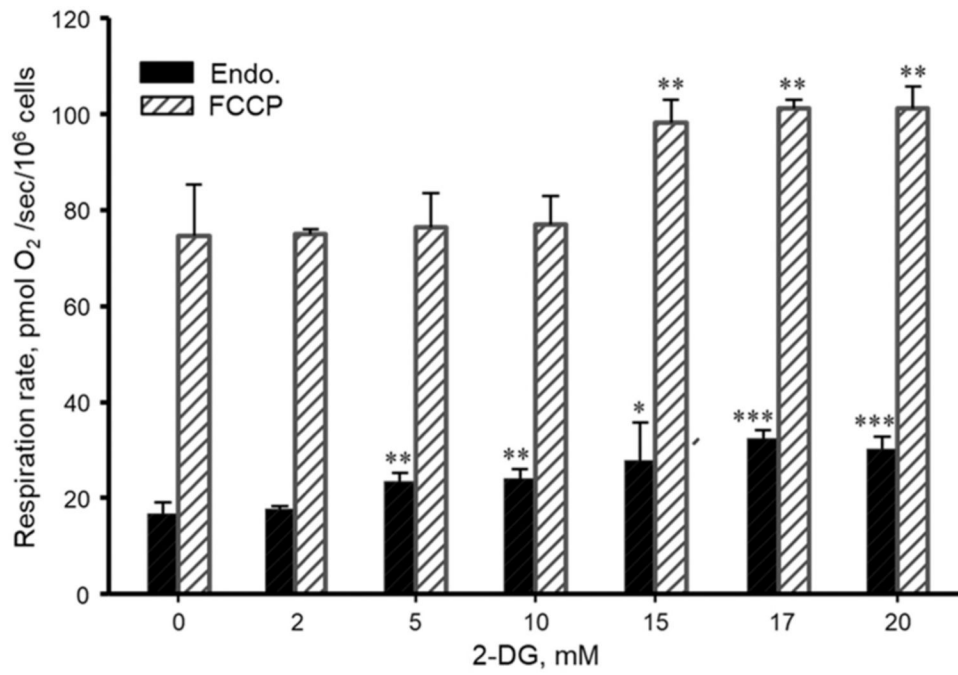A: Control. B: After 2-DG treatment (16 mM, 48 h).

Fig. 3.
Concentration-dependent effects of 2-DG on mitochondrial endogenous (Endo.) and uncoupled (FCCP) respiration rates in DLD-1 cells. *$P < 0.05$, **$P < 0.01$, ***$P < 0.001$ vs. control. $N = 3$ per group.
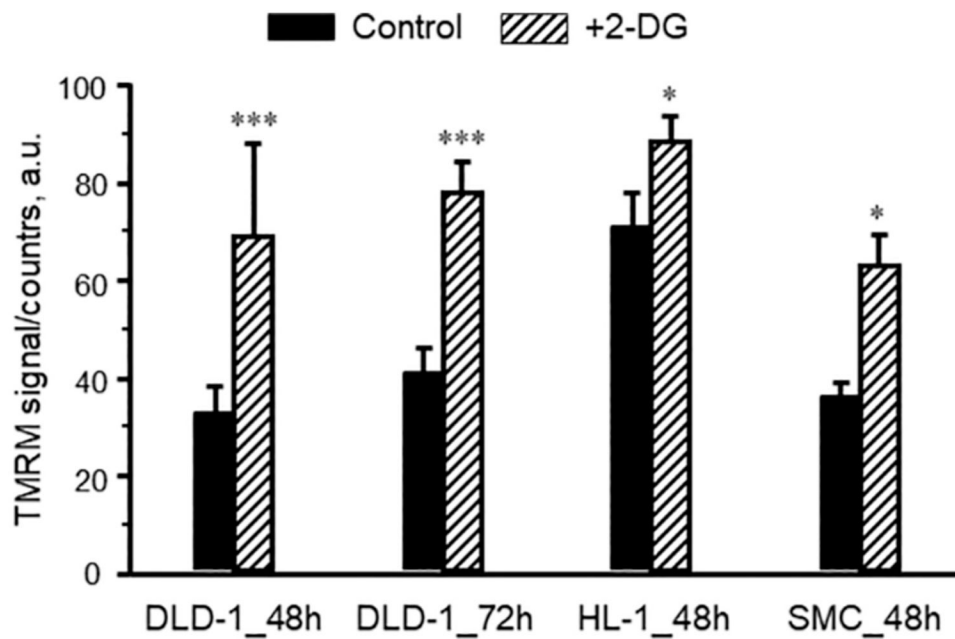
Fig. 4.
Flow cytometry analysis of Ψ_m in control and 2-DG-treated DLD-1, HL-1, and SMC cells. Results are presented as the TMRM fluorescence intensity (a. u.) in control (untreated) and after incubation with 2-DG (16 mM, 48 h). $*P < 0.05$, $***P < 0.001$ vs. control. $N = 3$ per group.
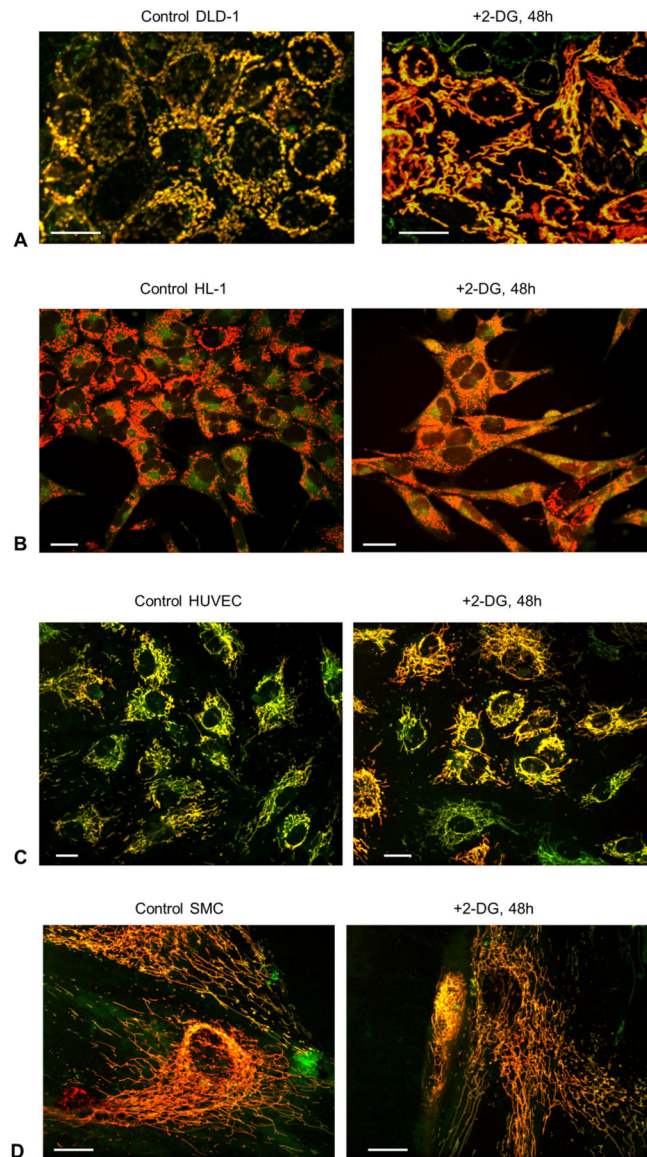
Fig. 5.
Representative fluorescence confocal mitochondrial images of control (A) and 2-DG-treated (16 mM, 48 h, B) cells. A, Changes of the mitochondrial arrangement after incubation of DLD-1 cells with 2-DG toward more mitochondrial network organization. B–D, No 2-DG effects on mitochondrial structure/organization were observed in HL-1 cells, HUVEC and SMC. Cells were preloaded with TMRM (0.1 μM) and MitoTracker Green FM (0.2 μM). Scale bars 20 μm.
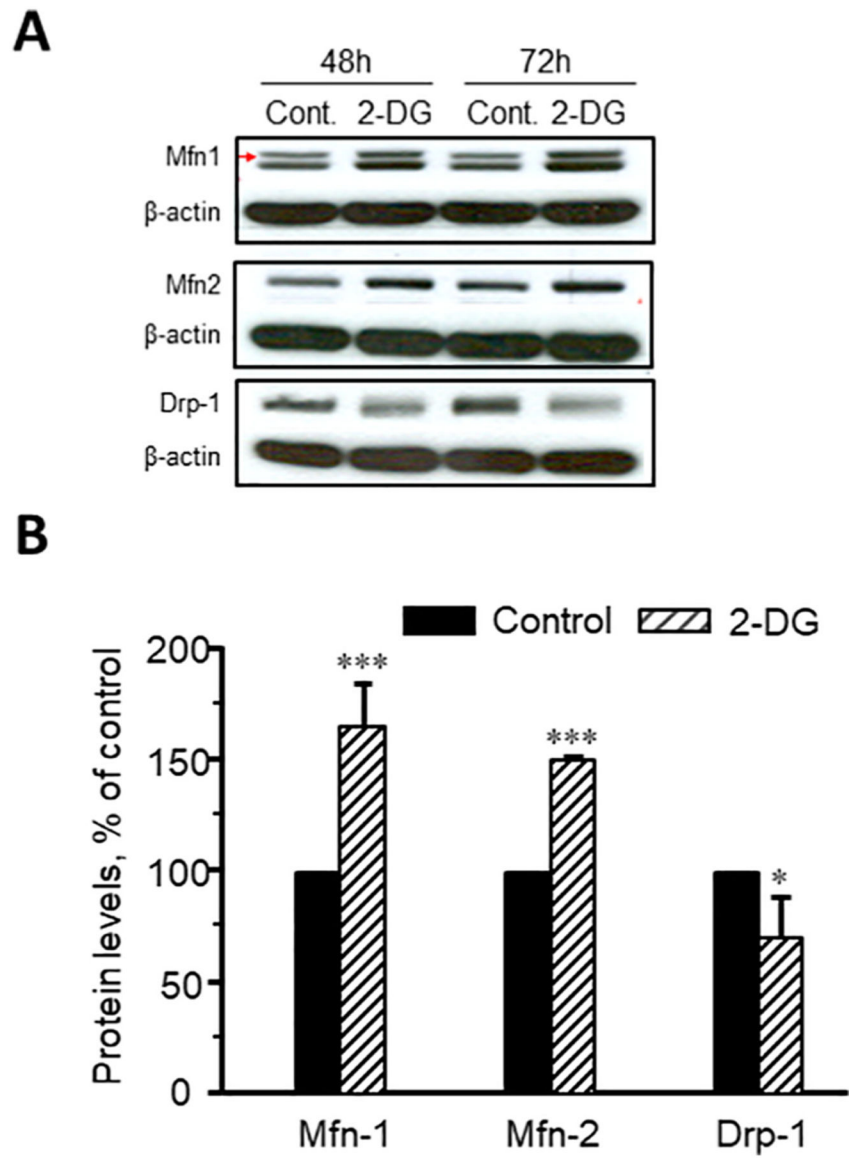
Fig. 6.
Representative immunoblots (A) and quantitative data (B) of expression of Mfn1, Mfn2, and Drp1 in DLD-1cells. $*P < 0.05$, $***P < 0.001$ vs. control. $N = 3$ per group.
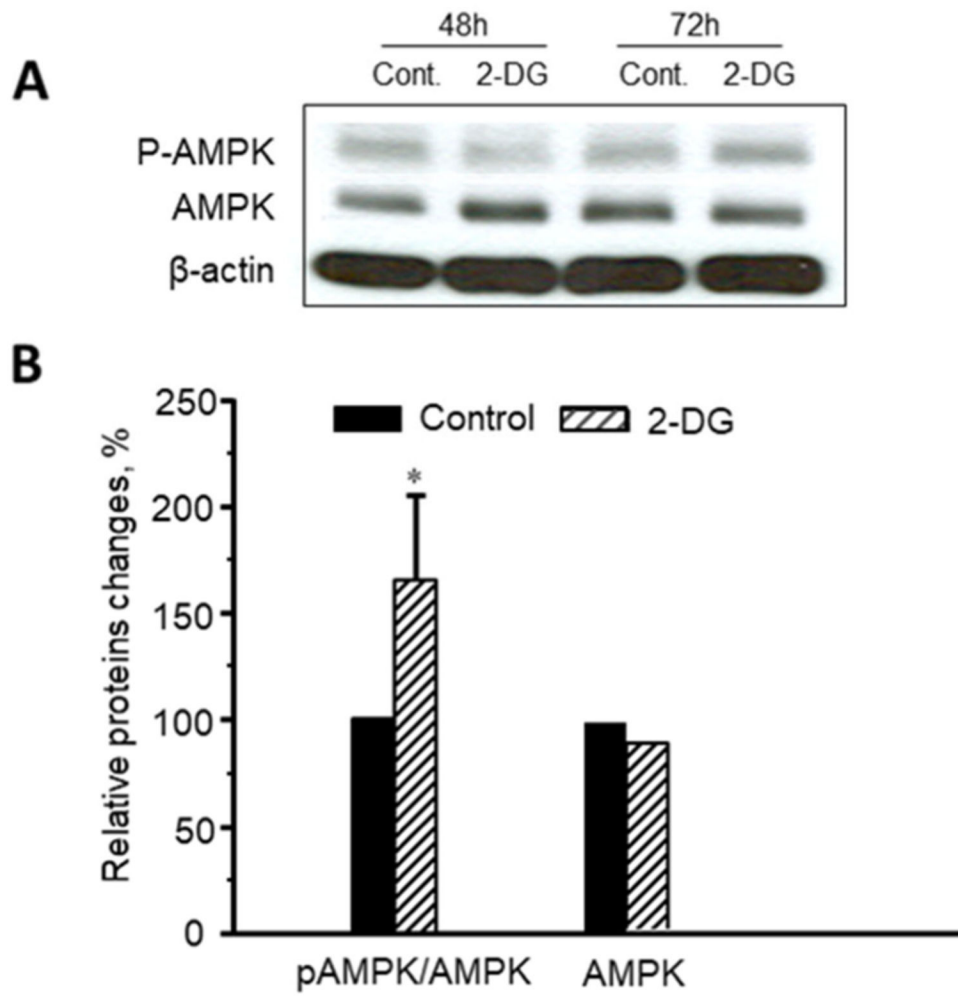
Fig. 7.
Activation (phosphorylation) of AMPK after 72 h incubation of DLD-1 cells with 16 mM 2-DG. *$P < 0.05$ vs. control. $N = 3$ per group.

Table 1

Citrate synthase activity in DLD-1, HL-1, HUVEC and SMC cells. The absence of 2-DG treatment (16 mM, 48 h) effects have been observed.

Cell type	DLD-1	HL-1	HUVEC	SMC
Control	0.036 ± 0.005	0.060 ± 0.01	0.040 ± 0.005	0.025 ± 0.002
2-DG, 16 mM, 48 h	0.037 ± 0.006	0.057 ± 0.01	0.045 ± 0.005	0.028 ± 0.004

CS activity is expressed in IU per 10^6 cells ($n = 3$).